

RESEARCH ON COMBUSTION PERFORMANCE IMPROVEMENT BY STRUT/WALL COMBINED INJECTION IN SCRAMJET COMBUSTOR

by

Junlong ZHANG*, **Guangjun FENG**, **Guowei LUAN**,
Hongchao QIU, and **Wen BAO**

School of Energy Science and Engineering, Harbin Institute of Technology, Harbin, China

Original scientific paper
<https://doi.org/10.2298/TSCI220917092Z>

Strut/wall combined fuel injection scheme was adopted to improve mixing and combustion efficiency in a scramjet combustor fueled with liquid kerosene in the condition of Mach 6. Injectors were placed on the front of the strut and the side wall of the combustor. A series of numerical simulations and experiments were carried out to improve the combustor performance under conditions of different incoming flow velocity, injection methods, and fuel distribution ratios. The value of pressure was obtained by pressure sensor and the flame images were captured by the high-speed camera in experiment. By processing and analyzing the basic data, characteristics of fuel mixing and combustion performance were discussed in this paper. Then, the influence mechanism of the strut/wall combined injection on the performance of the combustor was explained based on the performance with influence factors. Results indicated that the mixing and combustion efficiency was related to condition, injection method, and nozzle arrangement. The strut/wall combined injection dispersed the heat release, which could reduce the pressure rise and total temperature. The fuel distribution ratio between the strut injection and wall injection is also a key factor affecting the performance of the combustor. These results in this paper are valuable for the combustion organization in the supersonic combustor and the improvement of the combustor performance.

Key words: *strut/wall combined injection, combustor performance, mixing efficiency, flame characteristics, scramjet combustor*

Introduction

The supersonic flight has become a research hotspot in the world today [1, 2]. Scramjets have the advantages of high specific impulse and fast speed, which has been widely investigated in many countries [3, 4]. The supersonic combustor is the key component of the scramjet, which determined the performance of the aircraft [5, 6]. Liquid kerosene is widely used as a propellant and coolant for scramjet engines due to its high calorific value and large heat sink [7, 8]. In the supersonic combustor, the higher incoming flow velocity cause the residence time of the kerosene very short and bring great difficulties to the mixing of the air and fuel, ignition and stabilization of the fuel in the combustor [9, 10]. Therefore, the

* Corresponding author, e-mail: junlongzhang1990@163.com

optimization of combustion stabilization and injection methods has become a key factor in enhancing combustion organization and improving combustion efficiency.

There are two main injection methods at present, which include intrusive injection and non-intrusive injection. Non-intrusive injection mainly relies on injectors installed on the wall of the combustor [11]. Its characteristics are simple structure, low resistance and low penetration depth, which will result in the poor mixing of kerosene and air [12, 13]. The intrusive injector can cause complex shock wave structure, which is beneficial to enhance the development of fuel in supersonic flow. At the same time, the intrusive injector increases the residence time of the fuel, which is beneficial to the establishment and development of the flame [14, 15]. The strut is one kind of intrusive injection methods and plays the important role of injector and flame stabilizer [16, 17]. The concentrated heat release of fuel combustion caused thermal blockage in the combustor and part of the combustor transform into the subsonic state, in which the flame forward phenomenon was induced based on strut injection [18, 19]. The flame propagation in the supersonic airflow disturbed the performance of the combustor under the coupling effect of combustion and flow [20]. In response to these problems, some scholars have proposed a method of combined hierarchical injection to reduce the concentration of thermal release [21, 22]. The performance of the supersonic combustor with multi-strut was studied to improve fuel distribution, which was greatly related to the distribution ratio and the position of struts [23, 24]. When the fuel equivalent ratio of the strut increases to a certain level, the wall fuel could be ignited by the central flame to form a wall flame and a large area of subsonic velocity formed behind the strut, which was more conducive to the flame propagation and diffusion [25, 26].

Previous studies have investigated different combined injection methods based on the flow field and combustion field characteristics. The fuel injection method directly determines the fuel distribution and mixing characteristics, preparing for stable combustion. Therefore, this paper continues to study the effect of the strut/wall combined injection on the performance of the supersonic combustor.

Experimental set-up

Experiments in this paper were carried out on the directly connected scramjet combustor test, which was shown in fig. 1. The test rig is mainly composed of the air supply system, air heating system, measurement and control system and gas regulation system. During the experiment, a thin strut is used as a flame stabilizer, and a plasma torch was used as an igniter. In order to obtain the flame characteristics of the combustion region, the position of the strut is designed as the visual part, in which the quartz glass is installed. A high-speed camera is used to take pictures of the flame through the visual part, its frame rate is 8000 frames per second, and its exposure time is 120 μ s. The pressure inside the combustor is mainly measured by pressure sensors installed on the side wall.

The physical model used in this paper to calculate the strut/wall combined injection characteristics is shown in fig. 2. The grid is processed by ICEM. Most of the grids are hexahedral grids, and the total amount is about 2 million. In order to meet the y^+ requirement, the first layer grids of the wall boundary layer is 0.1 mm, and a gentle over-treatment is adopted for different grid sizes. The grids of the strut, nozzle holes and wall are encrypted.

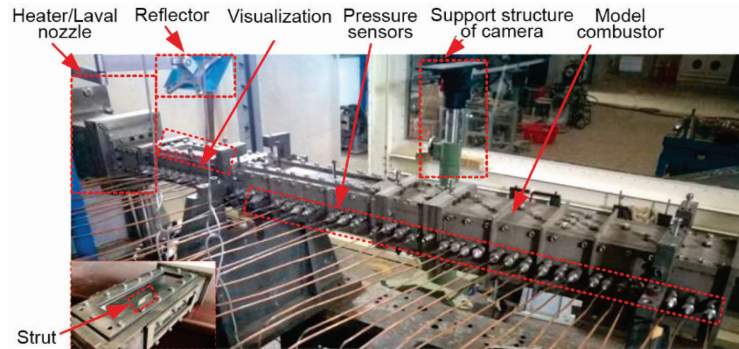


Figure 1. Photograph of the experimental system

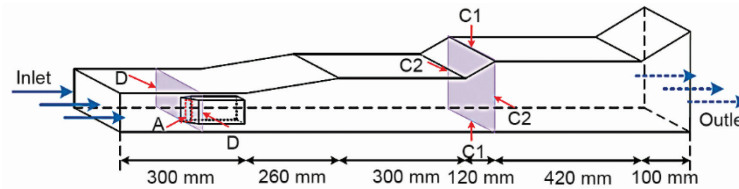


Figure 2. The physical model in numerical simulations

A Navier-Stokes solver was provided to calculate the flow field surrounding the combustor model. The governing compressible RANS equations were discretized using the finite volume framework. The governing RANS equations of continuity, momentum and energy were coupled together using the density-based solver. The renormalization group k - ε turbulence model was employed in this paper. And the governing equations are shown in:

– Continuity equation:

$$\nabla(\rho\vec{v}) = 0 \quad (1)$$

– Momentum conservation equation:

$$\nabla(\rho\vec{v}\vec{v}) = -\nabla p + \nabla(\bar{\tau}) + \rho\vec{g} + \vec{F} \quad (2)$$

– Energy conservation equation:

$$\nabla[\vec{v}(\rho E + p)] = \nabla\left(\sum_j h_j \vec{J}_j\right) + S_h \quad (3)$$

– Component transport equation:

$$\nabla(\rho\vec{v}Y_i) = \nabla\vec{J}_i + R_i + S_i \quad (4)$$

– The k -equation:

$$\frac{\partial}{\partial x_i}(\rho k u_i) = \frac{\partial}{\partial x_j}\left(\alpha_k \mu_{\text{eff}} \frac{\partial k}{\partial x_j}\right) + G_k + G_b - \rho\varepsilon - Y_M + S_k \quad (5)$$

– The ε -equation:

$$\frac{\partial}{\partial x_i}(\rho\varepsilon u_i) = \frac{\partial}{\partial x_j}\left(\alpha_\varepsilon \mu_{\text{eff}} \frac{\partial \varepsilon}{\partial x_j}\right) + G_{1\varepsilon} \frac{\varepsilon}{k}(G_k + C_{3\varepsilon} G_b) - G_{2\varepsilon} \frac{\varepsilon^2}{k} + S \quad (6)$$

A no-slip and adiabatic boundary condition was imposed along the solid walls by setting the velocity components to zero and nullifying the energy contributions of the wall faces to the dissipative fluxes. The viscosity and thermal conductivity were evaluated using a mass-weighted mixing law. The accumulation of errors in numerical simulation was evaluated by the method of error estimates from Smirnov [27, 28], which have made sure the accuracy of the simulation results.

Results and discussion

Analysis of the strut/wall combined injection characteristics

Fuel distribution in combustor with different injection methods

In this section, the Euler-Lagrange method is used to carry out the numerical simulation research on the strut injection and wall injection in the supersonic high-enthalpy incoming flow. The supersonic inflow velocity is $Ma = 2.8$ and the total temperature is 1680 K.

Figure 3 shows the distribution of the kerosene droplet size and the kerosene vapor under the supersonic high-enthalpy inflow condition. It can be seen that after the kerosene is injected into the combustor, the size of kerosene droplets decreases significantly. With the fragmentation of kerosene, the mass fraction of kerosene vapor gradually increases, which proves the evaporation process of droplets mainly occurs in this region. With the development towards the mainstream, the kerosene droplets distributed in the periphery gradually decrease, and the kerosene vapor gradually expands outward.

Figure 4 shows the distribution of the kerosene particle size and kerosene vapor in the supersonic combustor based on the strut injection. The number of kerosene particles decreases sharply after leaving the strut, and the penetration depth gradually decreases. At the end of the strut, there forms a low-speed recirculation zone due to the blocking effect of the strut. The low-speed recirculation area is distributed in the narrow space, which has a strong entrainment effect on the flow field near the center, and gradually weakens the interference to the peripheral flow field. The existence of the low-speed recirculation area has a certain entrainment effect on the mainstream and kerosene vapor. The kerosene diffusion boundary is far away from the low-velocity recirculation region, and the entrainment effect received is small.

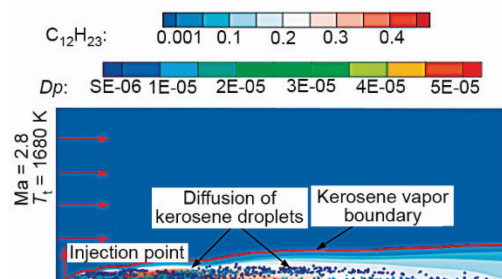


Figure 3. The diffusion of particle size and kerosene vapor with wall injection

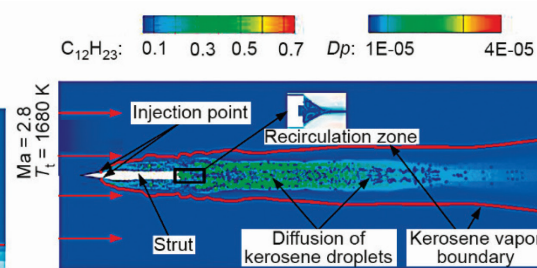


Figure 4. The diffusion of particle size and kerosene vapor with strut injection

The penetration depth and the variation trend of wall injection and strut injection were compared under the condition of the same injection momentum ratio. Figure 5 shows the penetration depth of kerosene based on strut injection increases rapidly at the initial injection position, and the penetration depth changes of both conditions are basically the same in the subsequent process. The kerosene injected based on the strut is separated from the strut at the position of 40 mm. The kerosene particles and the kerosene vapor are entrapped by the flow field and shrink toward the center of the flow field after breaking away the strut, and the penetration depth of the kerosene vapor changes relatively smoothly. The entrainment process lasted for a range of about 40 mm. The penetration depth continued to increase after that, and finally the gap between the two was not obvious.

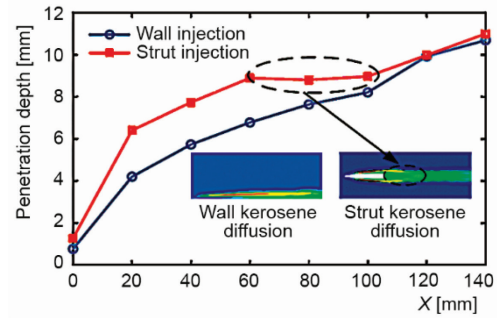


Figure 5. Penetration depth comparison of the strut/wall injection

Analysis of fuel mixing efficiency with strut/wall combined injection

In this section, 3-D CFD simulations of cold flowing field were used to discuss the influence of wall injection position and the distribution of fuel on the mixing under different incoming flow and injection conditions. The strut/wall combined injection parameters are shown in tab. 1. A is the strut injection, D, is the wall injection by the right and left wall on the same cross section as A, C1 is the wall injection by the upper and lower wall on the section C, C2 is the wall injection by the right and left wall on the section C. These injection positions are shown in fig. 2. The total pressure of injection is 2 MPa and the kerosene temperature is 600 K.

Table 1. The strut/wall combined injection parameters

Case	Ma	Injection method	Strut ER	Wall ER
1	4	A+C2	0.4	0.6
2	4	A+C1	0.4	0.6
3	5	A+C2	0.5	0.5
4	5	A+C1	0.5	0.5
5	6	A	1	0
6	6	A+D	0.5	0.5
7	7	A	1	0
8	7	A+D	0.5	0.5

Figure 6 shows the total pressure loss coefficient of the combustor under different conditions. It can be found that the injection process is mainly divided into two parts, the strut injection region and the wall injection region. The change of kerosene injection method has

little effect on the total pressure loss of the combustor for the same incoming flow state, and the total pressure loss increases with the increase of Mach number. Under the lower Mach number conditions ($Ma = 4/5$), the kerosene injected by the strut mixes with the main incoming flow behind the strut, and the total pressure loss gradually increases. The wall injection significantly increases the total pressure loss along the combustor. Under the higher Mach number conditions ($Ma = 6/7$), all kerosene is injected at the position of 270 mm, the total pressure loss values of the four conditions are similar. The total pressure loss is mainly caused by the mixing of the kerosene and the mainstream with total kerosene injection.

Figure 7 shows the mixing efficiency of kerosene and mainstream in the combustor under different conditions. It can be seen that the mixing process is also divided into two parts, the strut injection region and the wall injection region. In the strut injection region, lower fuel equivalence ratio has the higher mixing efficiency. The higher fuel equivalence ratio takes a longer distance to achieve the same mixing efficiency of kerosene and mainstream. Incoming flow conditions have little effect on the mixing efficiency in the combustor. In the wall injection region, the kerosene is injected into the combustor at the position of 980 mm. The mixing efficiency decreases rapidly and the main reason is that a large amount of gaseous kerosene gathers at this position. Then, the mixing efficiency continues to increase due to further mixing of the kerosene and the mainstream along the combustor. The mixing efficiency of Case 6 and Case 8 is the highest, which use the combined injection of the strut and coaxial wall. The advantage is that the injection of kerosene has been completed at 270 mm. The kerosene has a long distance and time to mix with the mainstream relatively, so its mixing efficiency is higher.

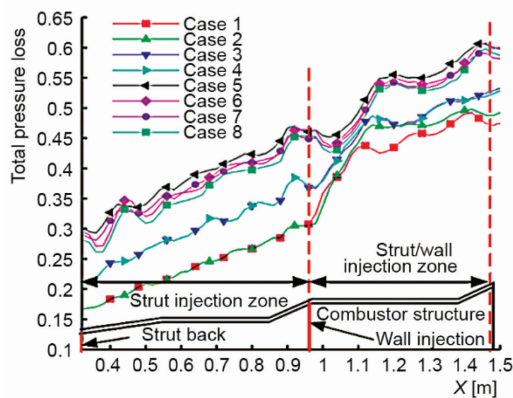


Figure 6. Total pressure loss of combustor under different conditions

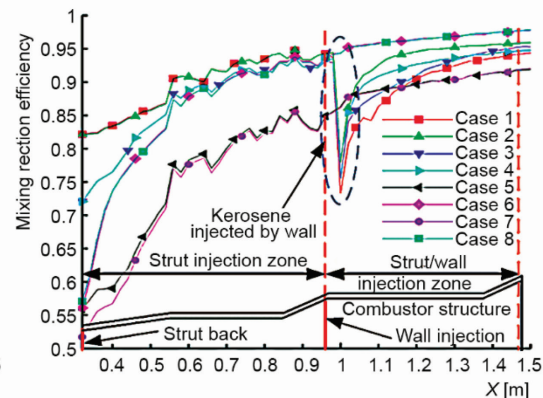


Figure 7. Mixing reaction efficiency of combustor under different conditions

Characteristics of combustion field with the strut/wall combined injection

In order to compare the effect of different strut/wall fuel distribution ratios on the flow field characteristics and combustion performance of scramjet combustor, the combustion field of different strut/wall fuel distribution ratios under the flight condition of Mach 5 is

calculated with 3-D CFD simulation. The fuel injection position of the strut is 355 mm, and the wall fuel injection position is 1090 mm, simulation conditions are shown in tab. 2.

Figure 8 shows the pressure distribution of combustor under different fuel distribution conditions. The distribution of combustion field is divided into strut kerosene combustion region and wall kerosene combustion region. When the strut injection equivalent ratio is 0.8, the pressure forward propagation in the isolator has affected the inlet incoming flow, and the inlet static pressure reaches 3 MPa, causing the inlet unstart. The pressure forward propagation does not affect the inlet incoming flow under the other three conditions. Using the strut/wall combined fuel injection can prevent the inlet unstart. Comparing the three strut/wall combined injection methods, the pressure forward propagation does not weaken with the decrease of the kerosene injected by the strut. When the total equivalent ratio is constant, the combustor stability margin can be improved under the strut/wall combined injection method only within a certain degree. The even fuel distribution on the wall of the strut has the highest combustion efficiency.

Table 2. The CFD simulation conditions

Case	Strut ER	Wall ER
9	0.8	0
10	0.5	0.3
11	0.4	0.4
12	0.3	0.5

Figure 8(b) is the comparison of wall pressure distribution under different combined fuel injection conditions. The pressure gradually increases as the fuel equivalent ratio of strut increases at the position of 300~800 mm. The pressure rise of strut decreases at the position of 800~1000 mm. The kerosene of wall is ignited and burned to generate a pressure rise after the position of 1000 mm. In short, the total pressure rise of combustor is based on the combined effect of the pressure rise generated by combustion of the fuel of strut and wall. A reasonable fuel distribution ratio between the strut and wall can effectively improve the performance of the combustor and the stability of the combustor.

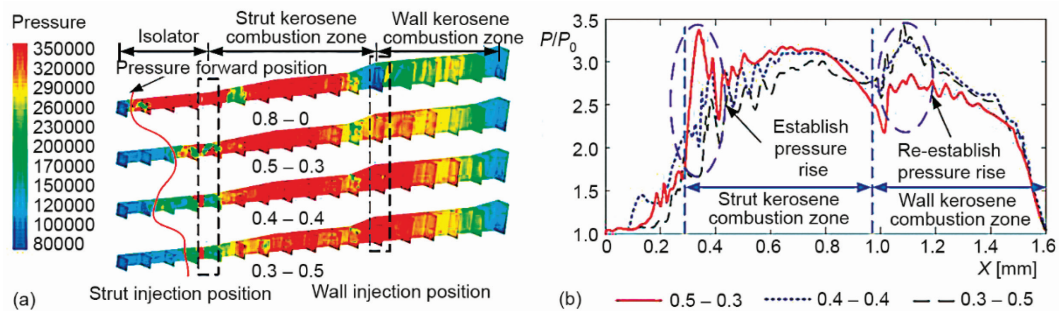


Figure 8. Pressure distribution of combustor under different fuel distribution ratios

Figure 9 shows the total temperature distribution in the combustor under different fuel distribution ratios. The kerosene combustion process in the combustion chamber can be divided into two parts, namely the strut kerosene combustion region and the wall kerosene combustion region. The kerosene combustion causes the increase of the total temperature. There is an obvious total temperature rise at the axial position of 400 mm, which indicates that the kerosene injected by strut is ignited and burned. The total temperature tends to be

stable at the axial position of 800 mm, the kerosene injected by strut is completely burned, and the heat of fuel is fully released. Because of adding the kerosene injected by wall, the total temperature rises again at the position of 1090 mm. At the outlet of the combustor, the total temperature difference is relatively small. The total temperature of Case 2 is relatively lower, which may be due to the little fuel injected by the wall and limited fuel penetration depth. Both of them make it not easy for the wall kerosene to contact of the strut flame, so the combustion is not sufficient.

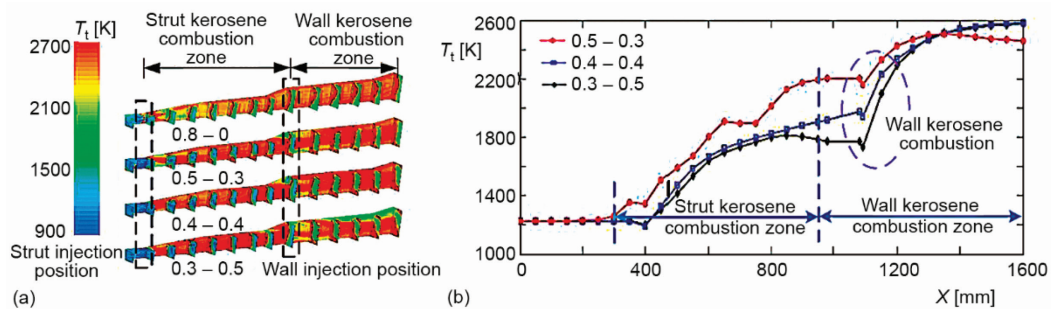


Figure 9. The trend of total temperature under different fuel distribution ratios

The fuel injection position determines the position of the combustion thermal release, and the fuel equivalent ratio determines the thermal release. The thermal released by combustion can cause a significant pressure rise. A large pressure rise blocks the flow of the mainstream flow in the combustor, which further leads to a series of problems. Therefore, a reasonable configuration of the injection position and equivalent ratio is an effective way to improve the performance of the combustor.

Performance evaluation of the combustor with strut/wall combined fuel injection

In order to further explore the influence of different strut/wall injection methods on the performance of the combustor, this section mainly analyzes parameters of the combustor through experiment. The conditions are different injection methods and strut/wall fuel distribution ratios.

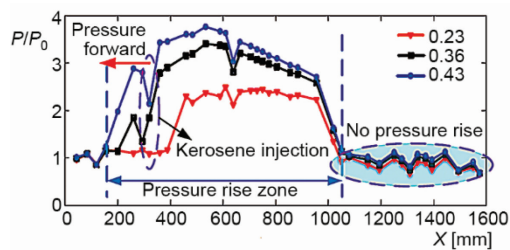


Figure 10. The pressure trend with different equivalent ratios

Stability of combustor under different injection methods

Three groups of ignition experiments of the strut injection in the combustor under different fuel equivalent ratios were carried out. The fuel equivalent ratios are 0.23, 0.36, and 0.43. Figure 10 shows the trend of pressure distribution under three different fuel equivalent ratios of the strut injection. It can be seen that when the fuel equivalent ratio is 0.23, the pressure at the position of 400 mm is not affected, and the highest-pressure ratio

reaches 2.4. When the fuel equivalent ratio reaches 0.43, the pressure disturbance has already affected the position of 185 mm. As the fuel equivalent ratio increases, the pressure gradually moves forward, causing the position of pressure disturbance gradually move forward. If continuing to increase the fuel equivalent ratio, it may cause unstable combustion of the combustor. Increasing the strut fuel equivalence ratio only builds up pressure rise in a certain area. After the position of 1050 mm, no pressure rise builds up, which seriously affects the performance of the combustor.

Figure 11 shows the trend of the static pressure of the wall in the combustor under different wall equivalent ratios when the equivalent ratio of the strut is 0.23. When the kerosene is injected by the strut and wall, there is pressure rise after the second expansion part due to wall kerosene combustion. When the kerosene injected by the strut is distributed to the wall, the equivalent ratio of the strut declines. Compared to the pressure rise in fig. 10, the pressure rise of the strut/wall combined fuel injection is smaller, and the position of pressure disturbance is more backward.

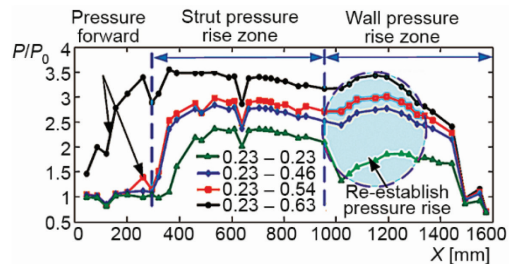


Figure 11. The wall pressure trend with different distribution ratios

When the wall equivalent ratio increases to 0.54, the position of pressure disturbance forward to $X=200$ mm. At this time, the total fuel equivalent ratio reaches 0.77, which is more than that of only the strut injection. But the impact of increased pressure on incoming flow with the strut/wall combined injection is smaller. When the wall fuel equivalent ratio increases to 0.63, the inlet of the isolator is disturbed, and the combustor can not work stably. Therefore, the strut/wall combined injection method can prevent the pressure rise to a certain extent, and reduce the back pressure gradient, which can increase the stable working range of the combustor.

Combustion performance with different injection methods

In order to explore the combustion characteristics in the supersonic combustor, several experiments were carried out under different the strut/wall injection conditions. Figure 12 shows the trend of total temperature along the wall in the combustor under different fuel equivalent ratios. It can be seen from the figure that the total temperature begins to rise at the position of 400 mm. The total temperature rises at the position of 400~660 mm is obvious, which indicates the main combustion region is in the expansion part of the combustor. In the first straight part, the total temperature of the equivalent ratio 0.23 tends to be stable, which proves that the kerosene has been fully burned at this position. With the equivalent ratio 0.36 and equivalent ratio of 0.43, the total temperature in the first straight part is still increased along the axial position. In the end, the three conditions have stabilized at the position of 1050 mm. The kerosene

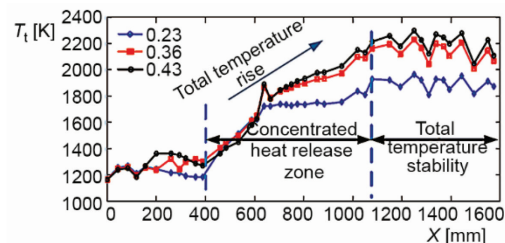


Figure 12. The total temperature trend with different equivalent ratios

injected by the strut has been fully burned, and the total temperature of the combustor gradually increases as the equivalence ratio increases.

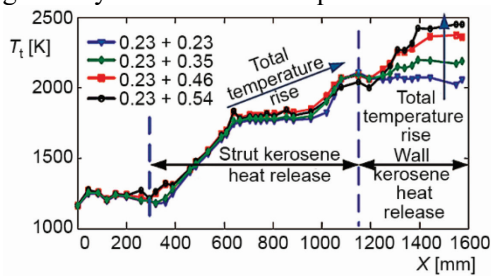


Figure 13. The total temperature trend with different equivalent ratios

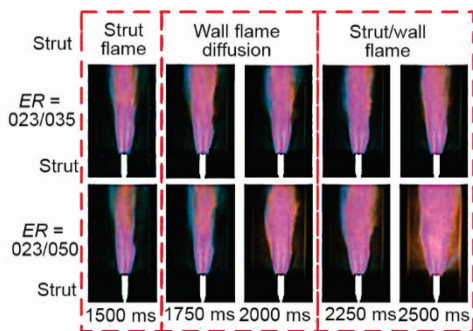


Figure 14. The flame shape changes with different equivalent ratios

The fuel equivalent ratio of the strut keeps constant, whose value is 0.23, and increasing the wall fuel equivalent ratio gradually is used to conduct an ignition test to evaluate the combustor performance under different wall kerosene equivalent ratios. Figure 13 shows the trend of total temperature in the combustor under different fuel distribution conditions. Before adding the kerosene injected by the wall, the total temperature of all conditions is basically the same, because of the same fuel equivalent ratio of the strut. Although the total fuel equivalent ratio is higher than that of the strut injection, the total temperature of the first straight part is relatively lower. When the kerosene is injected by the wall, the total temperature gradually rises with the wall injection equivalent ratio increasing.

The flame images from 1500 ms to 2500 ms are selected to analyze flame shape, which are shown in fig. 14. When the fuel equivalent ratio is 0.23/0.35, the flame shape does not change obviously. There is only a local flame behind the strut, and the flame area is relatively smaller. When the fuel equivalent ratio is 0.23/0.50, the flame shape changes greatly with the injection of wall fuel. The

central flame spreads to the wall, which can ignite the kerosene injected by the wall, and a global flame is formed downstream of the strut. The intensity of the combined injection flame and the flame shape are related to the fuel distribution ratio, and the establishment of the wall flame has an important effect on the enhancement of the central flame. Reasonable distribution of the fuel distribution ratio between the wall and strut can improve the combustor performance based on increasing the stability of the combustor.

Conclusions

Characteristics of strut/wall combined injection in the scramjet combustor were numerically and experimentally investigated. By comparing the mixing characteristics and combustion performance under different strut/wall fuel equivalent ratios, combustion characteristics and influencing factors of combined injection in the supersonic combustor were analyzed. The main conclusions are as follows.

- Fuel mixing characteristics were investigated in both strut/wall combined fuel injection scheme. The strut/wall combined injection method has higher mixing efficiency than the strut only injection method. Eight fuel injection cases with different fuel equivalent ratio between fuel injection and wall injection were numerically tested, among with the averaged distribution of the strut/wall showed the best fuel mixing performance.

- The combustion performance of scramjet combustor could be optimized by the strut/wall combined injection scheme. Thermal release caused by the strut fuel injection results in a significant increase of pressure in the region of $x < 1000$ mm, while no pressure rising appears in the region of $x > 1000$ mm. The wall fuel injection could lead to a wall combustion down stream of strut pressure rising region, improving the combustion efficiency in the whole combustor to a certain degree.
- The mechanism of combustion performance improvement by strut/wall combined injection scheme were researched. The fuel injection position and equivalent ratio determines the position of combustion thermal release and the mass of thermal release. As the wall fuel equivalence ratio increases, the flame spreads more easily to form global flame. The strut /wall combined injection is beneficial to slow down the heat concentration and improve the combustion efficiency of the combustor.

Acknowledgment

This research work is supported by the National Natural Science Foundation of China (Grant No. 12102110).

Nomenclature

ER – equivalence ratio, [–]
Ma – Mach number, ($= v/c$) [–]
 P – wall pressure, [MPa]

P_0 – base pressure, [MPa]
 T_t – total temperature, [K]
 X – flow direction coordinate, [mm]

References

- [1] Ognjanovic, O., et al., Numerical Aerodynamic-Thermal-Structural Analyses of Missile Fin Configuration During Supersonic Flight Conditions, *Thermal Science*, 21 (2016), 6B, pp. 3037-3049
- [2] Zhao, F., et al., Study of Linear Ablative Rate of D6AC Steel Wing Used on Supersonic Missile, *Thermal Science*, 23 (2019), 6B, pp. 4107-4116
- [3] Chang, J. T., et al., Research Progress on Strut-Equipped Supersonic Combustors for Scramjet Application, *Progress in Aerospace Sciences*, 103 (2018), Nov., pp. 1-30
- [4] Yang, P., et al., Experimental Study on the Influence of the Injection Structure on Solid Scramjet Performance, *Acta Astronautica*, 188 (2021), Nov., pp. 229-238
- [5] Qin, J., et al., Thermal Management Method of Fuel in Advanced Aeroengines, *Energy*, 49 (2013), Jan., pp. 459-468
- [6] Huang, W., et al., Survey on the Mode Transition Technique in Combined Cycle Propulsion Systems, *Aerospace Science and Technology*, 39 (2014), Dec., pp. 685-691
- [7] Chen, M. T., et al., Study on Influence of Forced Vibration of Cooling Channel on Flow and Heat Transfer of Hydrocarbon Fuel at Supercritical Pressure, *Thermal Science*, 26 (2021), 4B, pp. 3463-3476
- [8] Zhang, S. L., et al., Thermal Management of Fuel in Advanced Aeroengine in View of Chemical Recuperation, *Energy*, 77 (2014), Dec., pp. 201-211
- [9] Feng, G. J., et al., Diffusion Characteristics of Liquid Kerosene with Heat Transfer in a Strut-equipped Supersonic Combustor, *Acta Astronautica*, 203 (2023), Feb., pp. 246-251
- [10] Kummitha, O. R., et al., Hydrogen Fueled Scramjet Combustor with a Wavy-Wall Double Strut Fuel Injector, *Fuel*, 304 (2021), pp. 121425
- [11] Zhu, L., et al., Effects of Spray Angle Variation on Mixing in a Cold Supersonic Combustor with Kerosene Fuel, *Acta Astronautica*, 144 (2018), Mar., pp. 1-11
- [12] Vijayakumar, V., et al., Computational and Experimental Study on Supersonic Film Cooling for Liquid Rocket Nozzle Applications, *Thermal Science*, 19 (2015), 1, pp. 49-58
- [13] Liu, C. Y., et al., Dynamics and Mixing Mechanism of Transverse Jet Injection into a Supersonic Combustor with Cavity Flameholder, *Acta Astronautica*, 136 (2017), July, pp. 90-100
- [14] Athithan, A. A., et al., Numerical Investigations on the Influence of Double Ramps in a Strut Based Scramjet Combustor, *International Journal of Engine Research*, 24 (2022), 5, pp. 332-341

- [15] Athithan A. A., *et al.*, The Combustion Characteristics of Double Ramps in a Strut-based Scramjet Combustor, *Energies*, 14 (2021), 4, pp. 831-840
- [16] Huang, W., Investigation on the Effect of Strut Configurations and Locations on the Combustion Performance of a Typical Scramjet Combustor, *Journal of Mechanical Science and Technology*, 29 (2015), 12, pp. 5485-5496
- [17] Zhu, S. H., *et al.*, Experimental Study on Flame Transition in a Two-Stage Struts Dual-Mode Scramjet, *Journal of Aerospace Engineering*, 30 (2017), 5, pp. 1-7
- [18] Bao, W., *et al.*, Dynamic Characteristics of Combustion Mode Transitions in a Strut-Based Scramjet Combustor Model, *Proceedings of the Institution of Mechanical Engineers Part G Journal of Aerospace Engineering*, 29 (2013), 5, pp. 1244-1248
- [19] Hu, J. C., *et al.*, Flame Transition in Dual-Mode Scramjet Combustor with Oxygen Pilot Ignition, *Journal of Propulsion and Power*, 30 (2014), 4, pp.1103-1107
- [20] Zhang, J. L., *et al.*, Flame Oscillation Characteristics in a Kerosene Fueled Dual Mode Combustor Equipped with Thin Strut Flameholder, *Acta Astronautica*, 161 (2019), Aug., pp. 222-233
- [21] Zhong, F. Q., *et al.*, Performance of Supersonic Model Combustors with Staged Injections of Supercritical Aviation Kerosene, *Acta Mechanica Sinica*, 26 (2010), 5, pp. 661-668
- [22] Kobayashi, K., *et al.*, Performance of a Dual-Mode Combustor with Multistaged Fuel Injection, *Journal of Propulsion and Power*, 22 (2006), 3, pp. 518-526
- [23] Manna, P., *et al.*, Liquid-Fueled Strut-Based Scramjet Combustor Design: A Computational Fluid Dynamics Approach, *Journal of Propulsion and Power*, 24 (2008), 2, pp. 274-281
- [24] Desikan, S. L., Kurian, J., Strut-Based Gaseous Injection into a Supersonic Stream, *Journal of Propulsion and Power*, 22 (2006), 2, pp. 474-477
- [25] Qiu, H. C., *et al.*, Research on Combustion Performance Optimization in Scramjet Combustor with Strut/Wall Combined Fuel Injection Scheme, *Aerospace Science and Technology*, 109 (2020), 106376
- [26] Zhang, J. L., *et al.*, Flame Interaction Characteristics in Scramjet Combustor Equipped with Strut /Wall Combined Fuel Injectors, *Combustion Science and Technology*, 192 (2019), 10, pp. 1863-1886
- [27] Smirnov, N., *et al.*, Accumulation of Errors in Numerical Simulations of Chemically Reacting Gas Dynamics, *Acta Astronautica*, 117 (2015), Dec., pp. 338-355
- [28] Smirnov, N., *et al.*, Hydrogen Fuel Rocket Engines Simulation Using LOGOS Code, *International Journal of Hydrogen Energy*, 39 (2014), 20, pp. 10748-10756